**Current Biology, Volume *34***

## Supplemental Information

# Evidence for convergence of distributed cortical processing in band-like functional zones in human entorhinal cortex

**Daniel Reznik, Daniel S. Margulies, Menno P. Witter, and Christian F. Doeller**

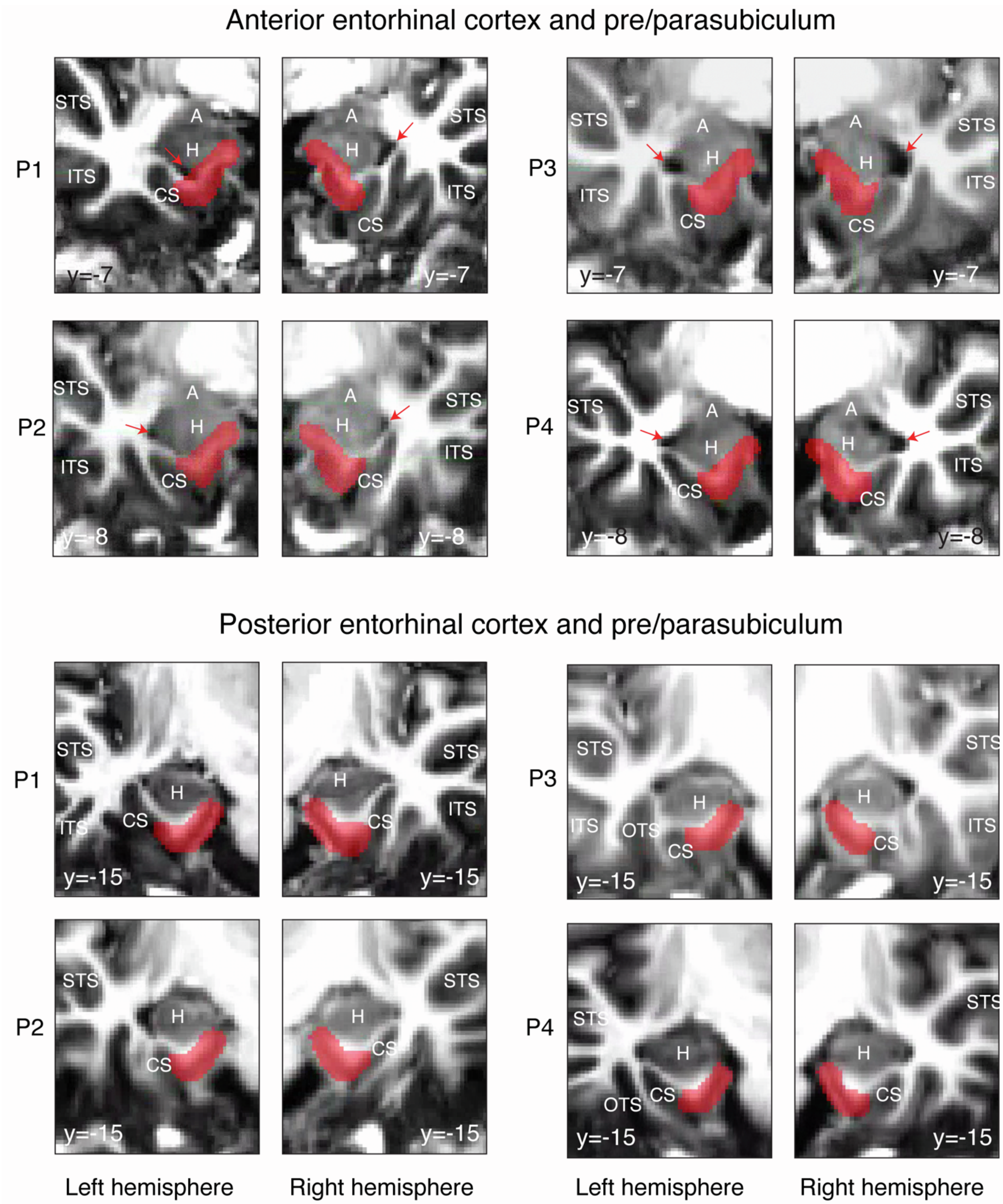
Anterior entorhinal cortex and pre/parasubiculum
P1
P2
P3
P4
STS
ITS
OTS
A
H
CS
y=-7
y=-8
Posterior entorhinal cortex and pre/parasubiculum
y=-15
Left hemisphere
Right hemisphere

**Figure S1. Parahippocampal gyrus masks. Related to Figure 1.**

We used a cortical mask of the parahippocampal gyrus that included the pre/parasubiculum and the entorhinal cortex. The masks were manually adjusted based on cytoarchitectonic studies and gross anatomical landmarks identified for each participant using their anatomical T1w images. The masks are presented in coronal slices (red color) for each participant in the anterior entorhinal cortex and pre/parasubiculum (top) and posterior entorhinal cortex and pre/parasubiculum (bottom). Red arrows in the anterior entorhinal cortex and pre/parasubiculum slices point to the beginning of the temporal horn of the lateral ventricle serving as the main landmark for identifying the ambient gyrus. A, amygdala; CS, collateral sulcus; H, hippocampus; ITS, inferior temporal sulcus; OTS, occipitotemporal sulcus; STS, superior temporal sulcus.

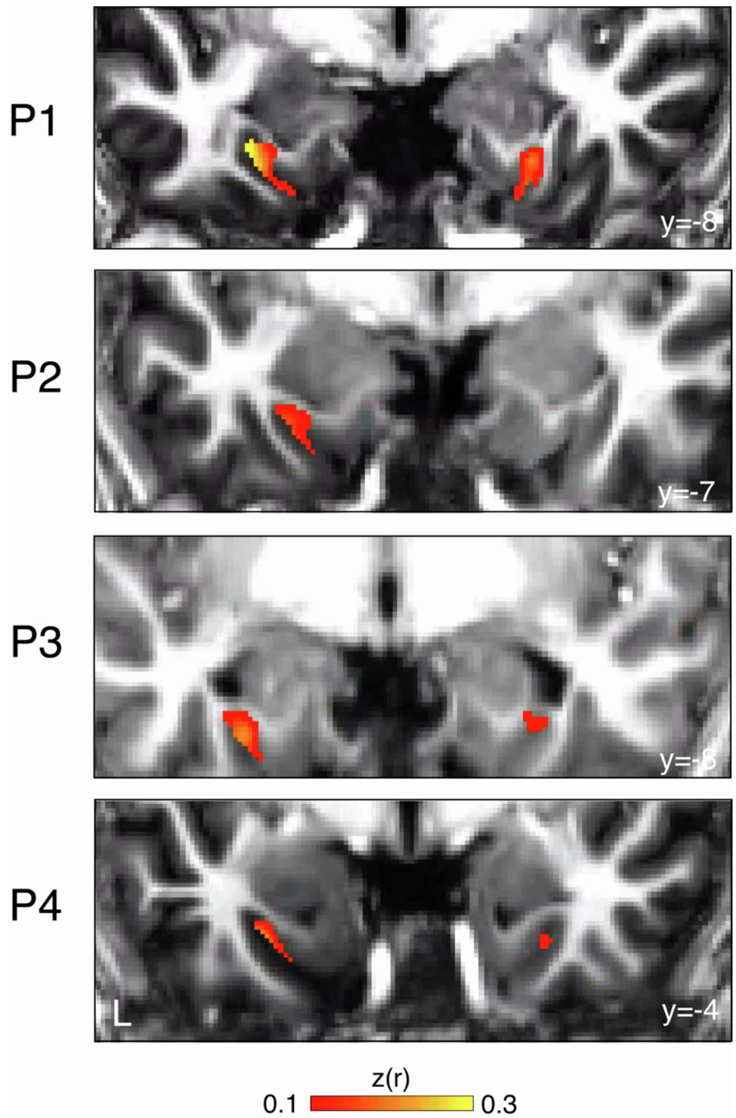


**Figure S2. Connectivity of the cortical network FPN-A with anterior MTL. Related to Figure 2.**

Connectivity of the cortical network FPN-A with anterior MTL revealed voxels located within the collateral sulcus, anatomically corresponding to the perirhinal cortex. Note that the peak correlation coefficients are located deep within the collateral sulcus, thus further supporting the association of this cortical network with the perirhinal cortex. L, left hemisphere.

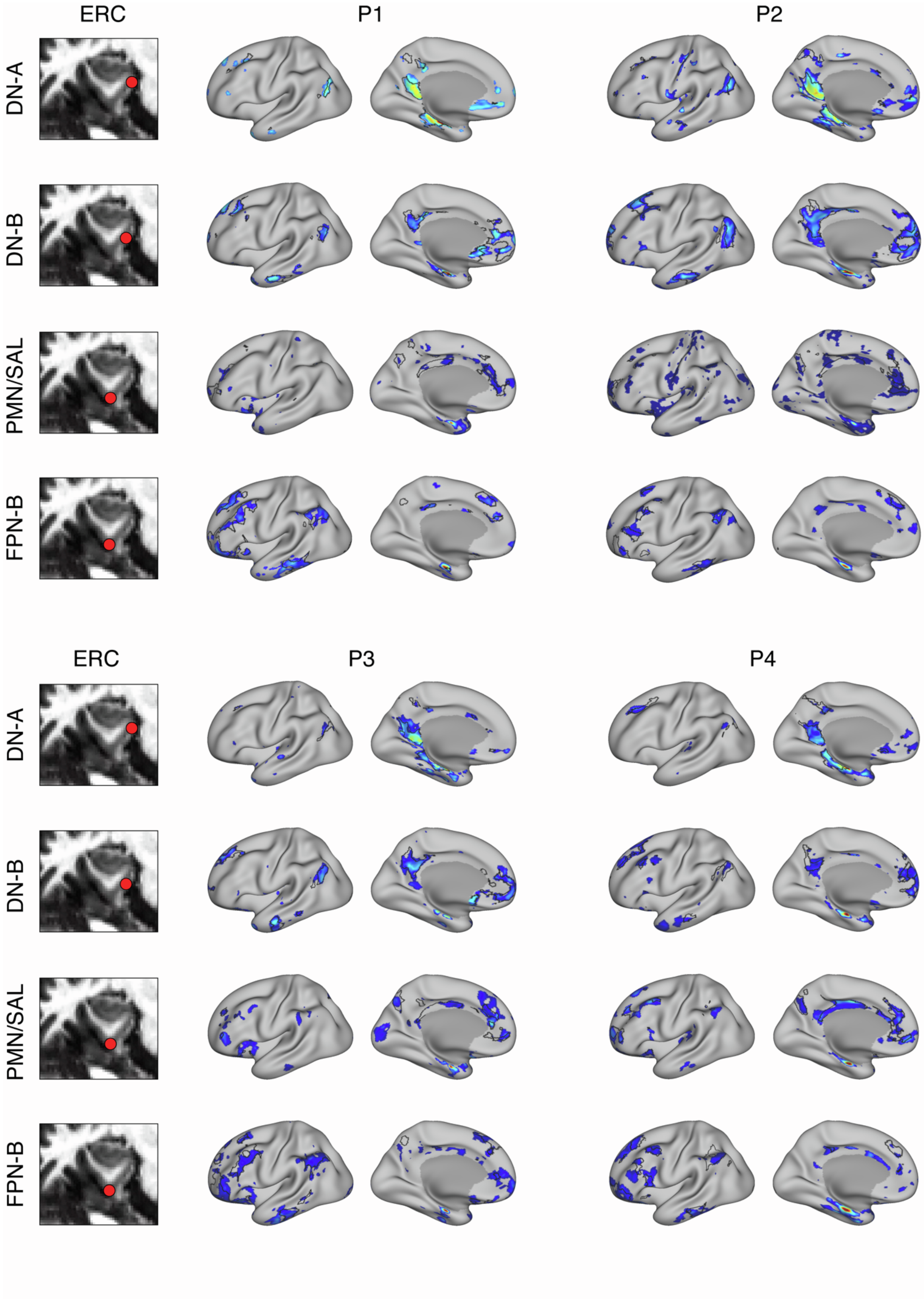

ERC
P1
P2
DN-A
DN-B
PMN/SAL
FPN-B
ERC
P3
P4
DN-A
DN-B
PMN/SAL
FPN-B

**Figure S3. Cortical connectivity patterns of distinct subregions of the entorhinal cortex. Related to Figure 2.**

To validate that subregions of the entorhinal cortex are associated with the corresponding cortical networks, in each participant, we computed Fisher z-transformed Pearson correlation coefficients between the entorhinal cortex voxels defined by the winner-takes-all procedure and the entire cortical mantle. Note that this procedure allowed the entorhinal cortex to be associated with the cerebral cortex in a “model-free” fashion, without imposing any network restrictions. The black outline on the cortical surface represents network boundaries defined by MS-HBM using network-estimation datasets. The representative locations of the entorhinal cortex voxels for each network are displayed in the volumetric image on the left. As can be seen from the figure, the entorhinal cortex correlation aligned well with the network boundaries, with the exception of PNM/SAL correlations in P2 which were nosier than in other subjects. Representative location of the entorhinal cortex seeds on the medial-lateral axis and the corresponding cortical network are presented to the left. Note that the representative entorhinal cortex seeds for the cortical networks PMN/SAL and FPN-B are located in the same lateral position to indicate their association with the most lateral parts of the entorhinal cortex; this entorhinal cortex seed position does not reflect the association of the cortical network FPN-B with the posterior portion of the entorhinal cortex anterior-posterior axis. See also Figure S4 for formal quantifications. ERC, entorhinal cortex.

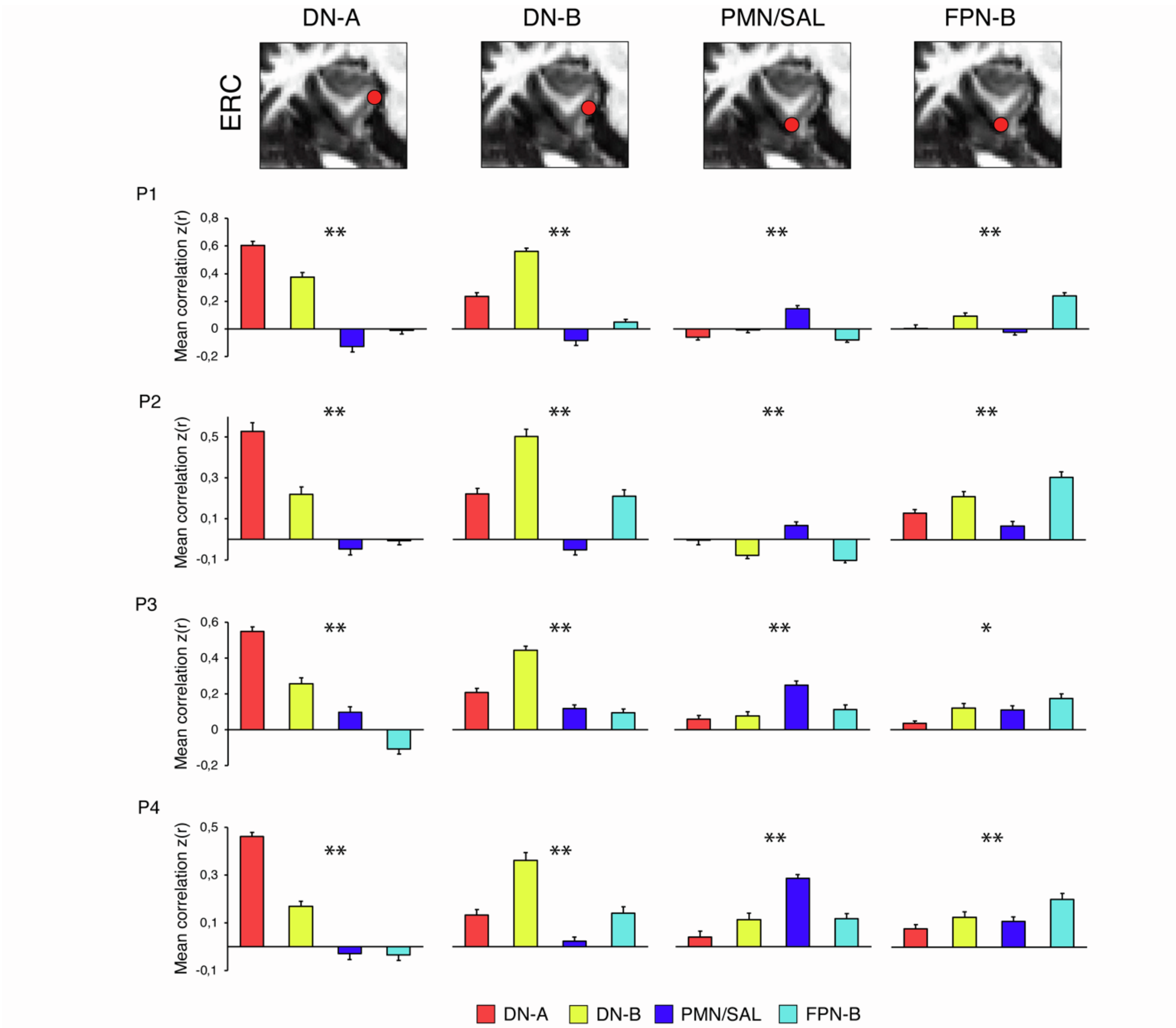


**Figure S4. Distinct subregions of the entorhinal cortex are preferably associated with the corresponding cortical networks. Related to Figure 2.**

Similar to Figure S3, but instead of visualizing the Fisher z-transformed Pearson correlation coefficients on the cortical surface, for each participant we quantified the correlation coefficients and compared them across different cortical networks using paired t-tests. All entorhinal cortex subregions preferably correlated with the time-series of their corresponding cortical network. * $p < 0.5$; ** $p < 0.01$; p-values represent the maximum p-value from all pairwise comparisons for each cortical network. Representative location of entorhinal cortex seeds on the medial-lateral axis and the corresponding cortical network are presented on the top. ERC, entorhinal cortex.

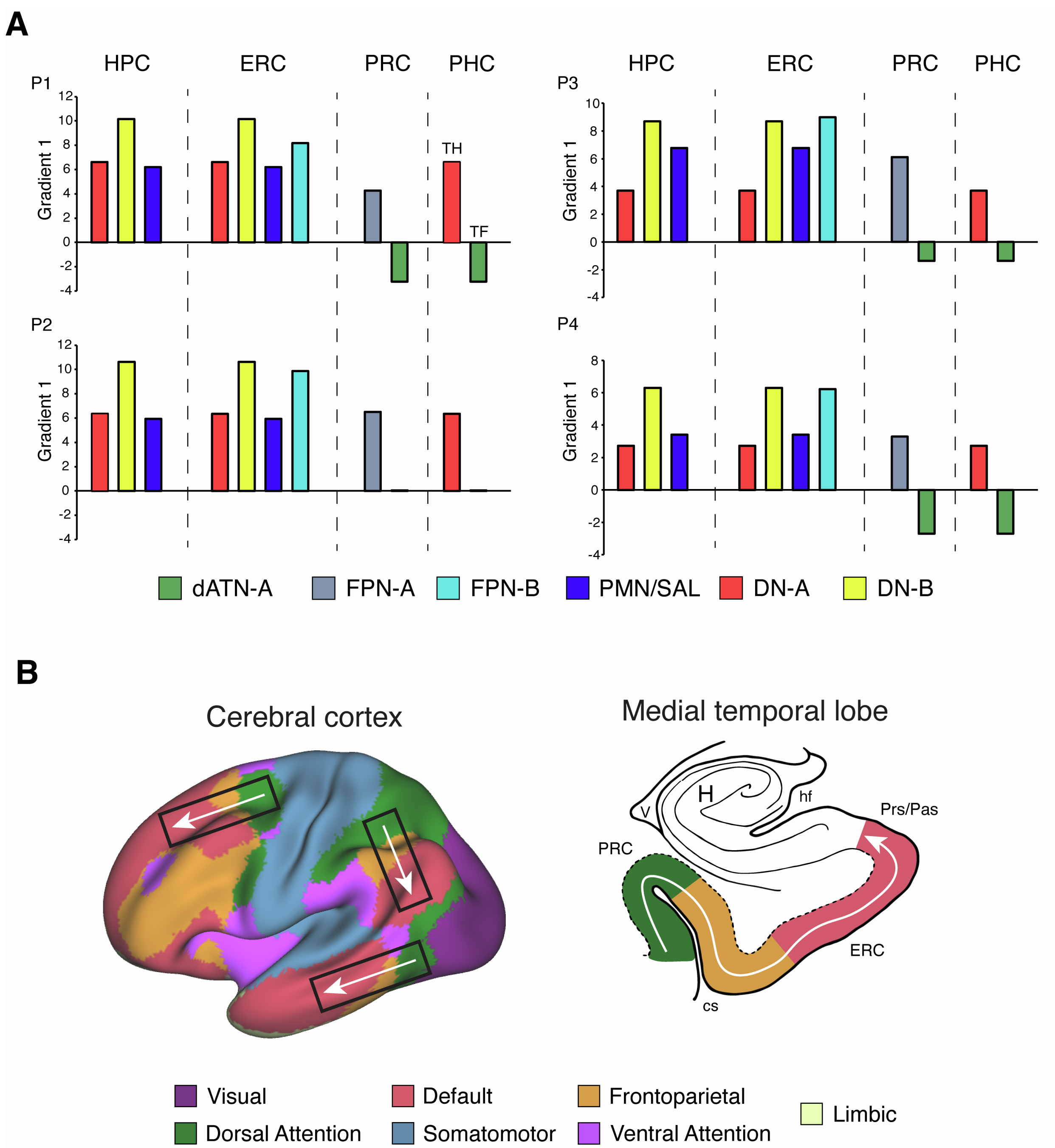
A
HPC
ERC
PRC
PHC
P1
P2
P3
P4
Gradient 1
TH
TF
dATN-A
FPN-A
FPN-B
PMN/SAL
DN-A
DN-B
B
Cerebral cortex
Medial temporal lobe
H
V
hf
Prs/Pas
PRC
ERC
cs
Visual
Dorsal Attention
Default
Somatomotor
Frontoparietal
Ventral Attention
Limbic

**Figure S5. Cortical convergence and mirrored cortical topography in human MTL, Related to Figure 4 and Figure 5.**

(A) Similar to main Figure 4, but instead of averaging the principal gradient values across all cortical networks associated with each subregion of the MTL, all separate cortical networks were considered. Note that the two cortical networks with the highest principal gradient values (DN-B and FPN-B) are associated with the entorhinal cortex, but not with the perirhinal or parahippocampal cortex. See discussion for more details. ERC, entorhinal cortex; HPC, hippocampus; PHC, parahippocampal cortex; PRC, perirhinal cortex; TF, parahippocampal area TF; TH, parahippocampal area TH.

(B) The order of the cortical networks associated with the entorhinal and the perirhinal cortex was consistent across participants – Dorsal Attention Network – Frontoparietal Network – Default Network (marked by a white arrow). Intriguingly, this order is repeatedly present throughout the human cortical mantle (colored using the 7-Network solution presented in Yeo, Krienen et al.[s1]). See Discussion for more details.

Supplemental reference

S1. Yeo, T.B.T., Krienen, F.M., Sepulcre, J., Sabuncu, M.R., Lashkari, D., Hollinshead, M., Roffman, J.L., Smoller, J.W., Zöllei, L., Polimeni, J.R., et al. (2011). The organization of the human cerebral cortex estimated by intrinsic functional connectivity. J Neurophysiol *106*, 1125–1165. https://doi.org/https://doi.org/10.1152/jn.00338.2011.